arXiv:1211.6720v1 [cond-mat.str-el] 28 Nov 2012

Wigner Crystallization in Electron-Hole Double Layers: Evolution from Long- to Short-Range Forces.

Benjamin M. Fregoso[1] and C. A. R. Sá de Melo[2]

[1] *Joint Quantum Institute and Condensed Matter Theory Center, Department of Physics,*
University of Maryland, College Park, Maryland 20742-4111, USA
[2] *School of Physics, Georgia Institute of Technology, Atlanta, Georgia 30332, USA*

We study fermions in two dimensions interacting via a long range $1/r$ potential for small particle separations and a short range $1/r^3$ potential for larger separations on length scales ξ. We computed the energy of the Wigner crystal and a homogeneous Fermi liquid phases in a variational approach and determined the phase diagram as a function of density and ξ at zero temperature. We discuss the collective modes in the FL phase, finite temperature effects on the phase diagram, and possible experimental realizations of this model.

PACS numbers: 71.10.Ca,71.10.Pm, 05.30.Fk

I. INTRODUCTION AND RESULTS

Inhomogeneity plays an important role in many highly correlated materials[1–8]. For example stripe phases which break translational symmetry of real space in one direction have been observed in high temperature superconductors[4]. Similarly, a Wigner crystal (WC) phase[1] which has only discrete translational symmetry of triangular lattices and six-fold rotational symmetry has been observed in electrons on the surface of Helium[2] and in ultra clean two dimensional hole gases[3].

For interactions which decay as a power law $1/r^\alpha$ the potential energy scales with density as $n^{\alpha/2}$ in two dimensions (2D) and the kinetic energy as n. The ratio of the potential to the kinetic energy scales as $n^{\alpha/2-1}$ which becomes $n^{-1/2}$ for Coulomb interactions, a constant for $1/r^2$ and $n^{1/2}$ for $1/r^3$ potentials. A stable WC crystal phase occurs when interactions are of the order of kinetic energy[1]. Hence a WC is expected in the high density regime or low density regime depending on the power law decay of interactions. For Coulomb forces this suggests that there is a phase transition at decreasing densities from a homogeneous Fermi liquid (FL) phase, which is conducting, to a WC phase, which is insulating. In this regime, perturbative methods fail thus one must resort to numerical studies[5,6].

In reality, many important systems do not have pure power law interactions. In two dimensional electron gases (2DEGs) in inversion layers or semiconductor quantum wells, the presence of a nearby gate modifies the Coulomb interaction. Image charges will form in the gates and they screen the interactions such that at short distances it is $1/r$ and at long distance is $1/r^3$ with a length scale given by the distance to the gate. The effects of such long-range forces dramatically changes the energetics of the 2DEG. A phase diagram was estimated in Ref.[7,8]. Recently the effects of long-range forces on superconductivity have been explored too[9]. A similar experimental scenario occurs in ionic liquid transistors[10] where an electrolyte is used as a dielectric in a standard field effect transistor configuration. Positive and negative charges accumulate at opposite ends of the electrolyte. Finally, recent progress in cooling techniques have allowed the study of degenerate dipole gases[11–14]. Such objects interact as $1/r^3$ at large separations. At short distances the interaction is modified by the interactions between the electronic clouds. The common feature of these systems is that there is a length scale in the interactions. They are composed of charges of opposite sign which are located in layers separated by a dielectric. As such, the interparticle potential crosses over between two different power law regimes.

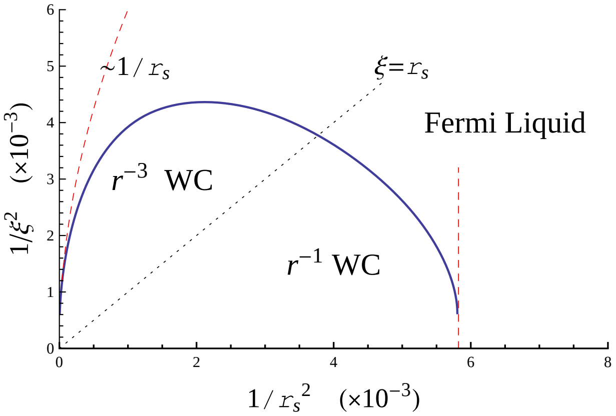

FIG. 1. (Color online) Phase diagram of spinless fermions in two dimensions with 43 particles showing the phase boundary between the Wigner crystal and uniform FL phases as function of the screening length ξ in units of a_0 and density $n = 1/(\pi a_0^2 r_s^2)$. Also shown is the $\xi = r_s$ line which divides the Coulomb $1/r$ regime (right) from the $1/r^3$ regime (left). The dashed(red) lines represent the analytical asymptotes of the boundaries (see text).

In this work, we study a minimal model in a variational approach of spinless fermions interacting with a $1/r$ ($1/r^3$) potential at short (long) distances in two dimensions, see Eq. 2. Our results agree with Ref.[7,8] in the study of 2DEG with a nearby gate, but we provide a *microscopic* model Hamiltonian from which the phase diagram arises. Moreover we find that this phase diagram should qualitatively describe other systems with similar crossover.

The corresponding zero-temperature ($T = 0$) phase diagram is presented in Fig. 1 as a function of the separation ξ and density n parametrized by $r_s = 1/(a_0\sqrt{\pi n})$. The FL and WC phases are indicated in the phase diagram and labeled according to the dominant interaction regimes. For fixed $\xi > \xi_c$ there is a regime of densities where the Wigner crystal is energetically more favorable than a uniform FL. We also show in dashed(red) lines the asymptotic forms of the phase boundaries from our numerical simulations. In the regime dominated by $1/r^3$ the asymptotic phase boundary corresponds to $\xi \sim r_s^{1/2}$, while in the Coulomb case it is $r_s =$ constant (~ 13). Intuitively, for $\sim 1/r^3$ potentials (left to the $\xi = r_s$ line) the kinetic ($\sim 1/r_s^2$) and potential energy $\sim e^2\xi^2/r_s^3$ are comparable when $\xi \sim r_s^{1/2}$, whereas for the $1/r$ regime, the potential energy scales as $\sim e^2/r_s$ and these energies are comparable when $1/r_s^2$ is a constant ($\approx 5.9 \times 10^{-3}$). Notice that there is a maximum value of $1/\xi_c^2$, corresponding to the condition $\xi_c \approx 15a_0$, below which the WC is more favorable for a wide range of r_s. The existence of the maximum is a general feature that follows also from the above physical argument; if ξ is too small the potential energy cannot be simultaneously of the same order as the kinetic energy. The limit $\xi \to \infty$ is *not* directly accessible with our method. Extrapolating we find that the FL phase is more stable than the WC phase for $r_s < 13$. For $1/\xi^2$ below the critical maximum and increasing density from zero to finite values, we find a first order phase transition from a 'dipolar' FL to a WC. With additional increases of the density beyond the $\xi = r_s$ line, the WC crosses over to a Coulomb WC. Upon further increase of the density, the WC phase transitions to a FL. This reentrant behavior for the FL phase is a remarkable characteristic of any 2D system interacting with an effective potential which crosses over from long to short-range. Fig. 1 constitutes one of our main results.

In what follows we show how this phase diagram is obtained. In section II we explicitly define the Hamiltonian and in section III we explicitly compute the energy of the homogeneous FL and discuss its collective modes as they are modified by the presence of ξ. In section IV we compute the energy in WC phase with a variational wave function. In section V we compare the energies of these two states in different density regimes and determine the ground state of the system. A discussion of the scaling of the WC energy with density is given along with a schematic finite temperature phase diagram.

II. MODEL

We start from a microscopic Hamiltonian

$$\hat{H} = -\sum_i \frac{\nabla_i^2}{2m} + \sum_{i<j} V(\mathbf{r}_i - \mathbf{r}_j), \tag{1}$$

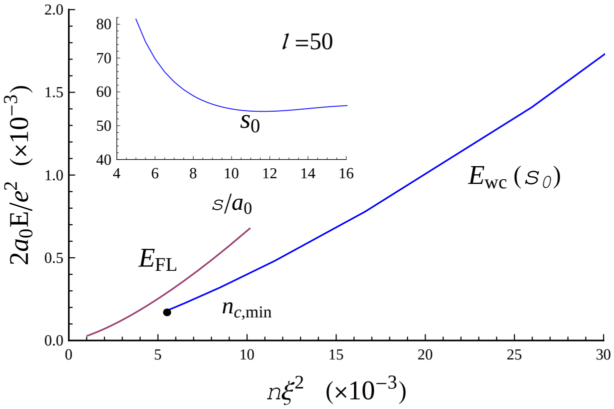

FIG. 2. (Color online) Energy per particle vs density (in units of particles per ξ^2) of the WC and FL phases. Here $\xi = 30a_0$. Inset: $\mathrm{E_{wc}}(s)$ vs size of the wave function.

where the first term corresponds to the kinetic energy and the second term

$$V(\mathbf{r}) = \frac{2e^2}{\epsilon r} - \frac{2e^2}{\epsilon(r^2+\xi^2)^{1/2}}, \tag{2}$$

describes the interactions of, say, electrons and their image charges located at the gate. The variable ξ is the 'screening' length and we treat it here as a phenomenological parameter. Physically it also could represent the classical effective dipole size. In the first case one would include the energy of the capacitor energy that forms between the gate and the 2DEG. However such effects are not considered here as they likely give small corrections to the mean field diagram[7,8]. ϵ is the dielectric constant of the medium. Note that for fixed density in the limit $\xi \to 0$ the interaction becomes $V(r) = 2e^2/\epsilon r$ twice the Coulomb potential whereas in the limit $\xi \to 0$ it becomes $V(r) = 2(e\xi)^2/\epsilon r^3$ to lowest non-vanishing order in ξ.

For both FL and WC phases, we consider a many-body ground state wave function to be

$$\Psi(\mathbf{r}_1, \mathbf{r}_2, ..., \mathbf{r}_N) = \mathcal{A}\left[\phi_1(\mathbf{r}_1)\cdots\phi_N(\mathbf{r}_N)\right], \tag{3}$$

where N is the number of particles, and $\mathcal{A}$ in a operator that describes the anti symmetrization necessary for indistinguishable fermions. Results for indistinguishable bosons and for classical distinguishable particles are straight forward extensions. For simplicity, we assume that the spin degrees of freedom are frozen, such that the wave function describing individual particles $\phi_\ell(\mathbf{r}_\ell)$ are either plane waves in the FL phase, or Gaussian centered at individual sites of a triangular lattice in the Wigner crystal phase.

III. FERMI LIQUID PHASE AND COLLECTIVE MODES

To begin, let us consider the homogeneous FL phase. Our system has two length scales. The first scale is ξ

while the second is the interparticle distance k_F^{-1} set by the density $n = k_F^2/(4\pi)$, where k_F is the Fermi momentum of the FL with Fermi energy $E_F = k_F^2/2m$. The relative size of these length scales determines the range of the potential. For $\xi/(a_0 r_s) \ll 1$ particles interact with a $1/r^3$ potential, whereas for $\xi/(a_0 r_s) \gg 1$ via the Coulomb $1/r$ potential, see Fig. 1. Explicitly, the energy per particle of a uniform polarized uniform FL is

$$\frac{E_{FL}}{E_0} = \frac{2}{r_s^2} + \frac{4\bar{\xi}}{r_s^2} - \frac{2}{\bar{\xi}}\Big[I_0(4\bar{\xi}/r_s) - I_2(4\bar{\xi}/r_s) + \frac{8\bar{\xi}}{\pi r_s} - 1 - L_0(4\bar{\xi}/r_s) + L_2(4\bar{\xi}/r_s)\Big], \quad (4)$$

where $\bar{\xi} = \xi/a_0$ is scaled by the Bohr radius $a_0 = \epsilon\hbar^2/me^2$, and the energy scale $E_0 = e^2/2a_0$. The functions $I_n(x)$ are the n^{th} order modified Bessel function of the 1st kind and $L_n(x)$ are the n^{th} order Struve functions. In obtaining Eq. (4), we used the fact that the two-body interactions shown in Eq. (2) have Fourier transform $V(q) = (4\pi e^2/\epsilon q)(1 - e^{-\xi q})$.

The first term in Eq. (4) is the kinetic energy and scales as the density n. The second term in Eq. (4) is the Hartree contribution, which also scales as n. In the limit $\bar{\xi} \to \infty$, $E_{FL}/E_0 = 2/r_s^2 + 4\bar{\xi}/r_s^2 - 32/(3\pi r_s)$ is formally divergent as interactions are long-range $1/r$. In a 2DEG the positive background charge cancels the Hartree term and in this case, $E_{FL}/E_0 = 2/r_s^2 - 32/(3\pi r_s)$, in agreement with known results[15]. The interaction term is twice that of a 2DEG, see our Eq. (2). The last term within the square brackets is the Fock contribution which becomes $-4\bar{\xi}/r_s^2 + 512\bar{\xi}^2/(45\pi r_s^3)$ as $\bar{\xi} \to 0$ and leads to $E_{FL}/E_0 = 2/r_s^2 + 512\bar{\xi}^2/(45\pi r_s^3) + O(\xi^4)$ in this $1/r^3$ regime. To $O(\xi)$ the Fock term cancels the Hartree term for pure $1/r^3$ potentials. Physically, the system behaves as charge neutral FL of dipoles. We note that including a background to enforce charge neutrality as in 2DEGs with $1/r$ potentials leads to negative energies and a self-bound system. In our case however, the energies are positive and the system has positive pressure. The energy of the uniform FL is shown in Fig. 2 for $\xi = 30a_0$.

A. Collective modes

The length scale ξ in the potential introduces important modifications to the collective excitations in the FL phase. The Fourier transform of Eq. (2) at zero momentum is well-defined, $V(0) = 4\pi e^2\xi$. This means that at sufficiently long distances the interaction is effectively short range $1/r^3$. This introduces important modifications to the energetics of the system[16]. For example, the Hartree and Fock terms must be included in the self energy to have a conserving approximation to the Green functions[17]. The collective modes are given by the zeros of the dielectric function $\epsilon(q,\omega) = 1 - V(q)\Pi(q,\omega)$. A non-conserving RPA calculation[18] gives a good approximation to the behavior of the collective modes. For an interaction of the form Eq. 2 we obtain,

$$\Omega_q = \left(\frac{4\pi\xi n e^2}{m\epsilon}\right)^{1/2} q. \quad (5)$$

This result is valid at weak interactions and small wave vectors. As we see, the system supports zero sound modes whose group velocity is proportional $\sim \xi^{1/2}$. The speed of the zero sound diverges as $\xi \to \infty$ which means that the power expansion in q/Ω breaks down. Indeed, the plasmon dispersion relation has been extensively studied in 2DEGs in GaAs[19,20] semiconductor quantum wells. The Fourier transform of the pure Coulomb potential $V(q) \sim 1/q$ diverges at zero momentum and leads to gapless $\sim \sqrt{q}$ mode dispersion[20].

According to the variational principle, the energy obtained using the many-body wave function described in Eq. (3) is a rigorous upper bound for the true ground state energy of the system. In the following analysis, we perform a variational calculation of the ground state energy of the Wigner crystal phase and compare it with that of the Fermi liquid phase obtained in Eq. (4).

IV. WIGNER CRYSTAL PHASE

In the Wigner crystal phase, the single particle wave functions are localized at sites i of a 2D triangular lattice, $\phi_i(\mathbf{r}) = (1/s\sqrt{\pi})\exp\left[-(\mathbf{r} - \mathbf{R}_i)^2/(2s^2)\right]$, where $\mathbf{R}_i$ is the site position and s parametrizes the 2D size of the wave function. These single particle wave functions are approximately orthonormal, since the overlap at different sites is exponentially small, $\int d^2r\, \phi_i^*(\mathbf{r})\phi_j(\mathbf{r}) = \exp\left[-(\mathbf{R}_i - \mathbf{R}_j)^2/4s^2\right] = \exp\left[-R_{ij}^2/(4s^2)\right]$, provided that the separation R_{ij} between sites i and j is much larger than the extent s of the single particle wave function, that is $R_{ij} \gg s$. We denote the lattice spacing by l and consider the regime of weakly ovelaping single particle wave functions, where $s < l/2$. The localized nature of the many-body wave function is reasonable only in this regime. Explicitly, the energy per particle in the WC phase is,

$$\frac{E_{\rm wc}(s)}{E_0} = \frac{1}{\bar{s}^2} + 2\int_0^\infty d\bar{k}\; (1 - e^{-\bar{\xi}\bar{k}})e^{-\bar{k}^2\bar{s}^2/2}F_1(\bar{k}) - \frac{\sqrt{2\pi}}{\bar{s}}\left(1 - e^{\bar{\xi}^2/2\bar{s}^2}\mathrm{Erfc}\big(\frac{\bar{\xi}}{\sqrt{2}\bar{s}}\big)\right)F_2(\bar{s}), \quad (6)$$

where the functions $F_i(y)$ are lattice sums given by $F_1(\bar{k}) = \sum_{i\neq j} J_0(\bar{k}\bar{R}_{ij})/N$ appearing in the second term of Eq. (6), and $F_2(\bar{s}) = \sum_{i\neq j} e^{-\bar{R}_{ij}^2/2\bar{s}^2}/N$ appearing in the third-term of Eq. (6). $\bar{s} = s/a_0$, $\bar{k} = ka_0$, $\bar{R}_{ij} = R_{ij}/a_0$ and J_n is the n^{th} order Bessel function of the first kind. The first term is the zero point motion due to the localization of the particles at the lattice sites. This term favors large single particle wave functions. The second and third terms are the Hartree-Fock (HF) contribution which is non-monotonic in s. The extension to particles with Bosonic statistics results in a change of the sign of the Fock term whereas for classical particles only the Hartree term is present.

We comment on the limiting behavior of Eq. 6. For $\xi \to \infty$ the system interacts with a Coulomb potential. In this limit,

$$\frac{E_{\rm wc}^{\rm Coulomb}}{E_0} = \frac{1}{\bar{s}^2} + \frac{\sqrt{2\pi}}{\bar{s}N} \sum_{i \neq j} e^{-\bar{R}_{ij}^2/4\bar{s}^2} I_0(\bar{R}_{ij}^2/4\bar{s}^2) - \frac{\sqrt{2\pi}}{\bar{s}N} \sum_{i \neq j} e^{-\bar{R}_{ij}^2/2\bar{s}^2}. \tag{7}$$

In the regime of non-overlapping wave functions $l/2s \gg 1$, the asymptotic form of the Bessel function $I_0(x) \sim e^x/\sqrt{2\pi x}$. As we see, the series in the second (Hartree) term diverges when $N \to \infty$ as expected since we have not included a neutralizing background charge. In this limit, taking a finite N gives a well defined energy which is non-monotonic in s. We find that this behavior extends to the $\xi \neq \infty$ regime and produces a WC state energy $E_{\rm wc}(s)$ that does not have a minimum as a function of s when the density is either too small or too large. On the other hand, in the limit of $\xi \to 0$ we obtain that the $O(\xi)$ contribution of the Fock term cancels the Hartree term (as in the FL phase) and the first non-vanishing term is $O(\xi^2)$. Since the resulting expression is not very illuminating, we omit it here.

V. DISCUSSION AND CONCLUSIONS

For $\xi \neq \infty$, the integrals appearing in the analytical expression of Eq. (6) need to be calculated numerically. We have computed numerically the energy per particle as a function of the density $n = 2/(l^2\sqrt{3})$ for the WC phase in a 2D triangular array of 43 and 55 particles. In Fig. (1) we show the resulting phase diagram for 43 particles, but we would like to emphasize that the qualitative behavior found is essentially unchanged with 55 particles. However, the calculation of the phase boundaries for the full range of parameters ξ and r_s is very intensive in the limit of large number of particles.

We establish the phase boundary between the solid and liquid phases by minimizing the energy in the solid phase with respect to the variational parameter s. A typical variation of the energy as a function s is shown in Fig. (2). When there is a local minimum of $E_{\rm wc}(s)$ located at $s = s_0$, we compare the energy $E_{\rm wc}(s_0)$ with the energy of the uniform screened FL with the same density. We find that the energy of the WC is always lower than the FL energy in the regime of tested values of ξ. However a local minimum of $E_{\rm wc}(s)$ does not exist for densities below a minimum $n_{c,min}(\xi)$ and for densities above a maximum $n_{c,max}(\xi)$, where the WC phase is unstable. This establishes that the WC phase is unstable for densities n satisfying the condition $n < n_{c,min}(\xi)$ and $n > n_{c,max}(\xi)$, in which case, the FL phase is the stable one. In the limit $\xi \to \infty$ and fixed density, we find that the critical value of density for the solid-liquid phase transition occurs when $r_s = 13$ in the case of 43 and changes little for 55 particles.

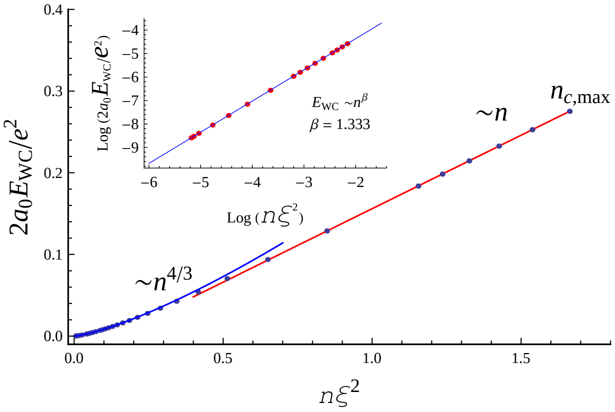

FIG. 3. (Color online) Scaling of the energy of the Wigner crystal (WC) near $n_{c,min}$ and $n_{c,max}$ for 43 particles. Here $\xi = 30a_0$.

A phase transition from a ferromagnetic FL to a ferromagnetic WC phase in a 2DEG is expected to occur for $r_s = 29$ according to recent Monte-Carlo simulations[6]. In the $\xi \to \infty$ limit we find such a phase transition for $r_s = 13$, but our interaction is twice that of pure Coulomb with finite size samples. We emphasize that our results does not apply in this regime as interactions are of pure Coulomb character and a neutralizing background charge must be explicitly considered along with numerical methods. Here we are interested in the regime of $\xi < \infty$ which we expect to be qualitatively correct.

It is interesting to note that in our simulations with 43 and confirmed with 55 particles the optimized energy values in the Wigner crystal phase can be fitted with a power law

$$E_{\rm wc} \sim n^{4/3} \tag{8}$$

for values of density close to the boundary with the FL phase, $n \to n_{c,min}^+$ in the regime of predominantly $1/r^3$ forces. See also Fig. 1. This is shown explicitly in Fig. 3 for $\xi = 30a_0$. Additionally, in the tested range of $20 < \xi/a_0 < 40$ we find that the exponent is 1.33 to within 1% error. Similar scaling behavior has been studied in 2DEGs with a screened $1/r^3$ potential *and* spin-orbit interaction[21]. Similarly the optimized energy in the Wigner crystal can be fitted by a linear power $E_{\rm wc} = C|n - n_{c,max}| + D$ for densities close to the FL phase $n \to n_{c,max}^-$, where C and D are constants but in the $1/r$ regime. In the tested range of $20 < \xi/a_0 < 40$, we find that the exponent is 1.00 to within 1% error.

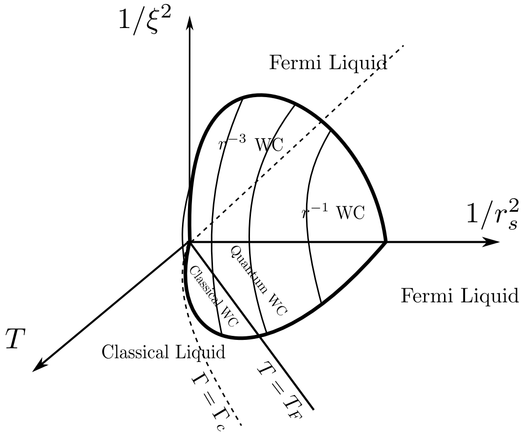

FIG. 4. Schematic variational phase diagram of the electron-hole double layer as function of density $\sim 1/r_s^2$, temperature T and layer separation ξ in appropriate units. Γ is the ratio of the potential to kinetic energy. See text for details.

A. Finite temperature mean field phase diagram of a screened 2DEG

Here we estimate the mean field phase diagram corresponding to a 2DEG in the presence of a nearby gate at finite temperature. As discussed above we assume this system can be modeled as an electron-hole double layer with separation ξ. The phase diagram in the $1/\xi^2$-density plane had been estimated before[7] from general considerations. At finite temperatures, we expect the melting of the WC to a liquid-like state (via Hexatic or bubble phases[8]). The limit $\xi \to \infty$ is not directly accessible with our method but can be estimated from general considerations[20]. In Fig. 4 we show the phase diagram in the $(T, n, 1/\xi^2)$ parameter space. In the $1/\xi^2 = 0$ plane the thermodynamics of the classical 2DEG is determined by the quantity Γ which is the ratio of the potential to the kinetic energy per particle. For a classical 2DEG this ratio is $\Gamma = (\pi n)^{1/2} e^2/T$. For $\Gamma < 1$ the kinetic energy dominates and the system behaves as a classical liquid. For $\Gamma \gg 1$ the Coulomb potential dominates and we expect a classical WC. The phase boundary is defined by $\Gamma = \Gamma_c \sim 100$, see Ref.[2].

For temperatures below $E_F \sim n \sim 1/r_s^2$ the Pauli principle and quantum correlations drive Γ down with increasing density[20], e.g., along the $1/r_s^2$ line in Fig. 4, $\Gamma \sim n^{-1/2}$ in the Hartree-Fock approximation. This defines a critical density above which $\Gamma < 1$ and a quantum fluid is recovered. The full melting line and the quantum/classical crossover in the plane $1/\xi^2 = 0$ is sketched in Fig. 4. Connecting the WC phases of the $1/\xi^2 = 0$ and $T = 0$ planes is a dome where a WC-like phase should be stable. Within this dome there exists at least 4 distinguishable phases corresponding to the quantum vs classical and $1/r$ vs $1/r^3$ regimes. Outside the dome there are only quantum and classical liquid-like phases.

In conclusion, we have obtained from a *microscopic* model, the phase diagram of fermions with an interaction which is smoothly deformed between two power law regimes which lie in the long-range and short-range category in 2D. We argue that such phase diagram is generic to any system with such crossover, e.g, 2DEG in semiconductor quantum wells with gates[7], and polarized dipole gases when the size of the dipoles is taken into account. Our results have relevance to experiments on polarized dipole gases in 2D where a WC is favorable at high densities. We suggest that at such high densities one likely should consider corrections to the $1/r^3$ form of the potential.

ACKNOWLEDGMENTS

We thank the JQI-PFC (BMF) and ARO (W911NF-09-1-0220) (CSdM) for support.

---

[1] E. Wigner, Phys. Rev. **46**, 1002 (1934).
[2] C. C. Grimes and G. Adams, Phys. Rev. Lett. **42**, 795798 (1979); E. Rousseau, D. Ponarin, L. Hristako, O. Avenel, E. Varoquaux, and Y. Mukharsky, Phys. Rev. B **79**, 045406 (2009).
[3] J. Yoon, C. C. Li, D. Shahar, D. C. Tsui, and M. Shayegan, Phys. Rev. Lett. **82**, 1744 (1999).
[4] S. A. Kivelson, I. P. Bindloss, E. Fradkin, V. Oganesyan, J. M. Tranquada, A. Kapitulnik, and C. Howald, Rev. Mod. Phys. **75**, 1201 (2003).
[5] B. Tanatar and D. M. Ceperly, Phys. Rev. B **39**, 5005 (1989).
[6] N. D. Drummond and R. J. Needs, Phys. Rev. Lett. **102**, 126402 (2009).
[7] B. Spivak, Phys. Rev. B **67**, 125205 (2003).
[8] B. Spivak and S. A. Kivelson, Phys. Rev. B **70**, 155114 (2004).
[9] S. Raghu, E. Berg, A. V. Chubukov, and S. A. Kivelson, ArXiv:1111.2982v1.
[10] R. E. G. III and M. D. Sherrill, Phys. Rev. Lett. **5**, 248250 (1960).
[11] M. Lu, N. Q. Burdick, and B. L. Lev, Phys. Rev. Lett. **108**, 215301 (2012).
[12] M. A. Baranov, M. Dalmonte, G. Pupillo, and P. Zoller, Chem. Rev. **112 (9)**, 50125061 (2012).
[13] K. Sun, C. Wu, and S. Das Sarma, Physical Review B **82**, 075105 (2010).
[14] C. Lin, E. Zhao, and W. V. Liu, Phys. Rev. B **81**, 045115 (2010).
[15] A. K. Rajagopal and J. Kimball, Phys. Rev. B **15**, 2019 (1977).
[16] J. P. Kestner and S. D. Sarma, Phys. Rev. A **82**, 033608 (2010).
[17] B. M. Fregoso and E. Fradkin, Phys. Rev. B **81**, 214443

(2010).
[18] L. P. Kadanoff and G. Baym, *Quantum Statistical Mechanics* (Benjamin, New York, 1962).
[19] M. Eriksson, A. Pinczuk, B. Dennis, C. Hirjibehedin, S. Simon, L. Pfeiffer, and K. West, Physica E **6**, 165 (2000).
[20] E. H. Hwang and S. D. Sarma, Phys. Rev. B **75**, 205418 (2007).
[21] E. Berg, M. S. Rudner, and S. A. Kivelson, Phys. Rev. B **85**, 035116 (2012).